Proceedings of the XVI National Conference on Superconductivity and Strongly Correlated Systems, Zakopane 2013

Influence of Iron Substitutions on the Transport Properties of $FeTe_{0.65}Se_{0.35}$ Single Crystals

V.L. Bezusyy, D.J. Gawryluk, A. Malinowski, M. Berkowski and M.Z. Cieplak
Institute of Physics, Polish Academy of Sciences, al. Lotników 32/46, 02-668 Warsaw, Poland

We study the *ab*-plane resistivity and Hall effect in the single crystals of $Fe_{1-y}M_yTe_{0.65}Se_{0.35}$, where M = Co or Ni ($0 \leq y \leq 0.21$). In case of each dopant two types of crystals, with different crystalline quality, are prepared by Bridgman's method using different cooling rates, fast or slow. The impurities suppress the superconducting transition temperature, T_c, with different rates. T_c reaches zero at markedly different impurity content: only 3 at.% of Ni, and about 14 at.% of Co. In addition, the suppression is somewhat dependent on the crystal cooling rate. The resistivity at the onset of superconductivity rises only weakly with the Co doping, while it increases 10 times faster for Ni. The Hall coefficient R_H is positive for Co doping indicating that hole carriers dominate the transport. For Ni R_H changes sign into negative at low temperatures for crystals with the Ni content exceeding 6 at.%. The implications of these results are discussed.

DOI: 10.12693/APhysPolA.126.A-76
PACS: 74.25.F–, 74.62.Dh, 74.70.Xa

1. Introduction

Recently, the iron-based superconductors (IS) have emerged as a new class of materials with superconducting mechanism likely related to spin fluctuations [1]. Many studies are devoted to tuning the properties of the IS by substitutions, either isovalent, expected to be potential scatterers, or heterovalent, leading to doping of carriers. However, since the IS are multiband materials, the effect of substitutions on the phase diagram may be quite complex. An example is the heterovalent substitution of the transition metals into Fe-site, which has been thoroughly researched in pnictides [2–4]. In $BaFe_2As_2$ such substitutions shift the Fermi level, but also reconstruct the Fermi surface [5]. The shift of the chemical potential, and also scattering by disordered impurities, are predicted by theoretical studies [6].

In the present work we study the transition metal substitutions into Fe-site in iron chalcogenides. While several such studies have been reported, they have been done for a limited impurity contents [7–9]. The $FeTe_{1-x}Se_x$ system is more complicated than $BaFe_2As_2$ for two reasons. First, two types of magnetic correlations exist throughout the phase diagram [10–12]. The parent compound $Fe_{1+\delta}Te$ shows the long-range antiferromagnetic (AFM) order with $(\pi, 0)$ wave vector, which is suppressed upon doping with Se. Instead, the (π, π) spin resonance emerges in the superconducting region, likely involved in the superconducting mechanism. However, in the intermediate region between the AFM and superconducting phases, the $(\pi, 0)$ magnetic fluctuations survive on a local scale, competing with superconductivity, and probably leading to incoherent scattering of carriers [12].

The second complication arises from inhomogeneities in the $FeTe_{1-x}Se_x$ crystals, which frequently grow either with the excess of Fe, or with Fe vacancies. The excess Fe occupies interstitial positions and magnetic clusters are formed around them, enhancing the $(\pi, 0)$ magnetic correlations and suppressing superconductivity [13]. The Fe vacancies may also cluster, forming inclusions of non-superconducting $Fe_7(Te\text{-}Se)_8$ phase [14].

The crystals of $FeTe_{1-x}Se_x$ with $x = 0.5$ are optimal for superconductivity. However, two tetragonal phases with slightly different Se content have been observed at this x [15]. On the other hand, it has been shown that the crystals with $x = 0.35$ may be grown as a single-phase material, and out of 18 elements that have been examined, only Co, Ni and Cu are properly substituted into the host matrix [16]. In the present study we therefore evaluate the influence of Co and Ni impurities on the transport properties of $FeTe_{0.65}Se_{0.35}$.

2. Experimental details

The single crystals of $Fe_{1-y}M_yTe_{0.65}Se_{0.35}$ with M = Co or Ni, and y up to 0.21, have been grown using Bridgman's method, as previously described [16]. Two batches of crystals have been prepared, using identical growth parameters except for the velocity of crystallization, equal to above 15 mm/h and 1.2 mm/h, which we call henceforth fast-cooled (FC) and slow-cooled (SC) crystals, respectively. These crystals are of different crystalline quality: while the cleavage plane is mirror-like in SC crystals, it is much inferior in the FC samples [14]. The quantitative point analysis, performed by energy dispersive X-ray (EDX) spectroscopy, shows that Co and Ni effectively substitute Fe and their contents are close to the nominal. The average Fe+M content is 0.99(3). The ratio Te:Se is also close to the nominal. X-ray powder diffraction indicates $P4/nmm$ tetragonal matrix with small amount of Fe_3O_4 and $Fe_7(Te\text{-}Se)_8$ phases, which are often present in such crystals [14, 16, 17]. High resolution transmission electron microscopy shows that $Fe_7(Te\text{-}Se)_8$ inclusions in SC crystals have larger size than the ones formed in FC crystals, although their volume fraction is the same [14].

The ac magnetic susceptibility is measured with magnetic field amplitude of 1 Oe and a frequency of 10 kHz in warming mode (field orientation has no effect on the

superconducting transition temperature, T_c). The transport properties are studied in the temperature range from 2 to 300 K using Physical Property Measurement System (Quantum Design) by four-probe method. The resistivity is measured in the *ab*-plane in zero magnetic field, and the Hall effect is studied by AC method and in the magnetic field up to 9 T, directed parallel to the *c*-axis.

3. Results and discussion

3.1. Resistivity

Figure 1 shows the T-dependence of the *ab*-plane resistivity ρ, normalized to resistivity at room temperature, ρ_{300}, for SC and FC crystals doped with Co and Ni. For both impurities the T_c decreases monotonically with increasing y for both types of crystals. However, the shape of ρ vs. T curve depends both on the impurity, and on the crystal type.

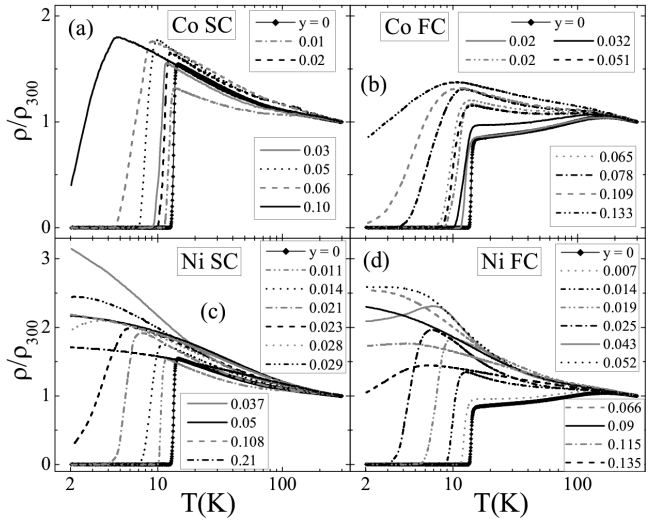

Fig. 1. The T-dependence of the *ab*-plane resistivity, ρ, normalized to the room temperature value, ρ_{300}, at zero magnetic field, for $FeTe_{0.65}Se_{0.35}$ crystals, SC-type doped with Co (a) and Ni (c), and FC-type doped with Co (b), and Ni (d).

In the FC samples with small y, the ρ/ρ_{300} below 150 K decreases with decreasing T, indicating good metallic character. With increasing y the dependences acquire low-temperature upturn, which on average increases progressively with increasing y, suggesting impurity-related origin. However, in Co-doped samples with small y ($y < 0.05$) the magnitude of the upturn shows considerable variation from crystal to crystal, and it may even differ for two samples with the same y, cut from the same crystal. This suggests that, in addition to impurity-induced effects, there is some other factor affecting resistivity. At $y > 0.05$ the variation disappears, presumably because impurity-related effects become dominant. In Ni-doped samples the variations of the upturn are considerably smaller, which may be a result of stronger impurity potential. Another difference between Co and Ni-doping is that in Co-doped samples the progressive growth of the upturn continues up to the highest values of y studied here. On the other hand, in Ni-doped crystals the resistance in the low-T limit saturates when y exceeds about 0.05, and starts to decrease for larger y. Such a decrease may indicate the reduction of the scattering of carriers, possibly by some type of magnetic ordering.

In SC samples the behavior is qualitatively different, because the low-T upturn exists in all samples, even for $y = 0$. Moreover, it changes only weakly with y. Thus, it appears that in SC crystals the other factors, impurity unrelated, strongly affect low-T transport. In fact, the large difference between FC and SC crystals is reflected in the susceptibility, as illustrated in the inset to Fig. 2 for two undoped ($y = 0$) samples. While the transition width is sharp in the FC crystal, it is very broad in the SC sample which indicates that the SC sample is more inhomogeneous.

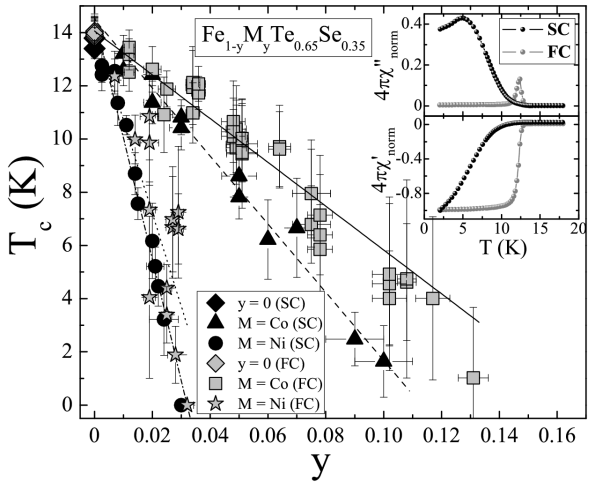

Fig. 2. T_c versus y for SC and FC crystals with Ni and Co impurities. The vertical error bars show 10% to 90% resistive transition width, while y and horizontal error bars are determined from EDX. The solid, dashed, dotted and dashed-dotted lines are guides to the eye showing the initial slope of superconductivity suppression for Co(FC), Co(SC), Ni(FC), and Ni(SC), respectively. The inset shows T-dependence of the imaginary part (top) and the real part (bottom) of AC magnetic susceptibility for undoped SC and FC crystals.

Figure 2 shows the dependence of T_c on y for the SC and FC crystals. Here T_c is defined as middle point of superconduction transition, and the vertical error bars reflect 90% to 10% transition width. The y values and the horizontal error bars show average impurity content and the standard deviations, respectively, obtained from several EDX measurements performed in different points on the crystal. All lines are guides to the eye showing the initial slope of SC suppression, dT_c/dy (in K/at.%), equal to about –0.82, –1.18, –3.46, –4.55 for Co(FC),

Co(SC), Ni(FC), Ni(SC), respectively. Thus, we observe that T_c decreases faster in SC crystals than in FC crystals, and that Ni suppresses T_c more effectively than Co. The faster decrease of T_c in SC samples is most likely caused by the small superconducting volume fraction. On the other hand, the stronger effect of Ni impurity occurs in both types of crystals, so it seems to be at least partially related to larger nominal valence of Ni impurity. However, if we now extract from the data the critical concentration y_c, at which T_c reaches zero in FC crystals, we find $y_c \approx 0.14$ (Co), and $y_c \approx 0.03$ (Ni). Assuming that T_c is suppressed by a rigid band shift of the density of states at the Fermi level by electron doping, the y_c's should differ by a factor of about two, whereas we find a factor of more than four. Thus, Ni-doping induces more complex effects, maybe involving strong localization by deep impurity potential, or some additional scattering.

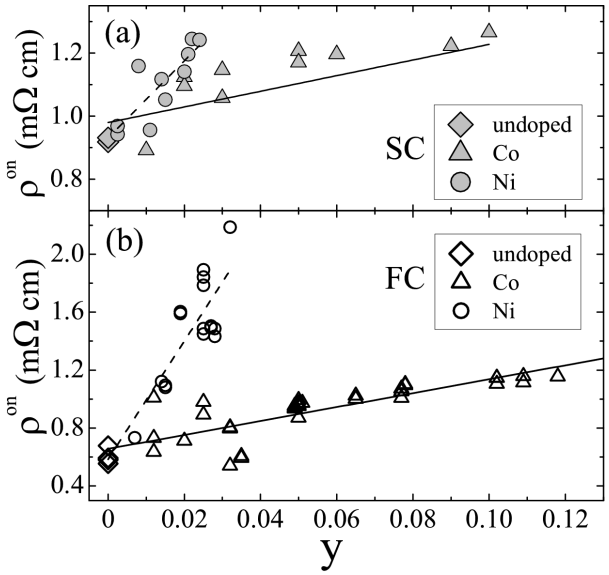

Fig. 3. ρ^{on}, resistivity at the onset of superconductivity (as defined in the text), versus y for SC (a) and FC (b) crystals. The linear fits to the data for Co and Ni are shown by solid and dashed lines, respectively.

It would be useful to compare the T_c suppression to the scattering rates induced by impurities. Unfortunately, the presence of upturn does not allow extracting the residual resistivity. Instead, from the data in Fig. 3, we extract the quantity ρ_{on}/ρ_{300}, where ρ_{on} is the value of the resistivity at the onset of superconductivity. To minimize the scatter of the data from imperfect measurement of the sample dimensions, we make use of the fact that ρ_{300} does not show any definite y-dependence, so that we can approximate it by the value averaged over various y, $\bar{\rho}_{300}$. Finally, we calculate $\rho^{on} \equiv (\rho_{on}/\rho_{300})\bar{\rho}_{300} \simeq \rho_{on}$, which is plotted versus y in Fig. 4 for SC and FC samples. The rates of the increase of ρ^{on} with increasing y, $d\rho^{on}/dy$ (in mΩ cm/at.%), are equal to about 0.05(1), 0.04(1), 0.29(3), and 0.12(2) for Co(FC), Co(SC), Ni(FC), and Ni(SC), respectively. It is clear that the rates are smaller in SC crystals. Close inspection of Fig. 3 reveals that this results mostly from larger values of ρ^{on} in the limit of small y in SC samples, which reflects the presence of large upturn, not related to impurities. On the other hand, the rates for FC crystals imply that the Ni impurity induces upturn by a factor of about 6 times larger than the Co impurity. This correlates with the strong suppression of T_c and confirms the conclusion that simple electron doping cannot explain the effects induced by Ni substitution.

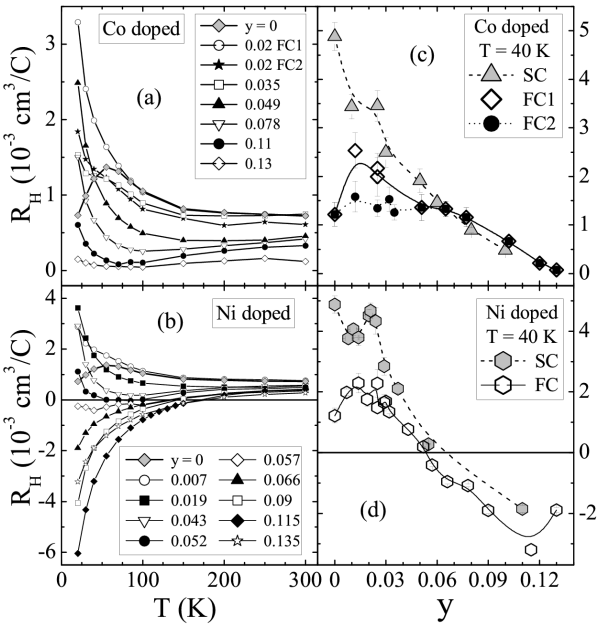

Fig. 4. (a)–(b) R_H versus T for FC samples, doped with Co (a) and Ni (b). (c)–(d) R_H at $T = 40$ K versus y for SC and FC samples, doped with Co (c) and Ni (d). In (c) FC1 and FC2 indicate data for samples with large and small upturns, respectively. All lines are guides to the eye.

3.2. Hall effect

Figure 4a,b presents the T-dependence of the Hall coefficient R_H for FC samples doped with Co and Ni impurities. In the $y = 0$ sample the R_H is positive, it rises as T is lowered down to about 50 K, and shows a downturn at lower T. With increasing y initially a low-T upturn in R_H appears. We stress that this upturn is very well correlated with the upturn observed in resistivity, reproducing sample-to-sample variations observed at small y in Co-doped crystals. As y increases further, the magnitude of R_H is reduced in the whole T-range, clearly pointing to the electron doping of the system. Nevertheless, the R_H remains positive for all y in Co-doped samples, indicating that the hole contribution to the conduction is dominant. On the other hand, in Ni-doped crystals the R_H at low T changes sign into negative when y exceeds 0.056, signaling stronger electron doping. The $R_H(T)$ dependences in case of SC crystals are similar, except for substantially larger low-T upturns at small y, correlated closely with the resistivity upturns.

The $R_H(y)$ dependences, measured at $T = 40$ K for SC and FC crystals, are compared in Fig. 4c,d. Since in Co-doped system large variation of upturns exists at small y, we plot in (c) two separate curves, for samples with large (FC1) and small (FC2) upturns. It is evident that for both impurities the R_H in the SC crystals is larger than in FC crystals, but the difference is restricted to region of small y. Similarly, the difference between FC1 and FC2 occurs for $y < 0.05$ only. Looking for the possible explanations of these upturns we note that similar low-T upturns have been observed for $FeTe_{1-x}Se_x$ crystals in the intermediate region between AFM and superconducting phase. They have been attributed to incoherent scattering of carriers from $(\pi, 0)$ magnetic fluctuations [12]. It is plausible that similar scattering affects transport in our crystals. While we find no excess Fe, the inclusions of nonsuperconducting $Fe_7(Te\text{-}Se)_8$ phase are detected, particularly well developed in the SC crystals [14]. The enhancement of magnetic fluctuations due to these inhomogeneities may contribute to additional scattering at small y.

The R_H is seen to approach zero in Co-doped samples at $y_{R_H} \approx 0.13$, while in case of Ni this occurs at half of this value, namely $y_{R_H} \approx 0.056$. This seems to be consistent with the expectation of the electron doping. Moreover, in the Co case we have $y_{R_H} \approx y_c$, suggesting that electron doping may suppress the T_c. On the other hand, for Ni impurity y_c is substantially smaller than y_{R_H}. This confirms that the effects of Ni substitution are more complex. This is further underscored by the observation that in Ni-doped crystals with $y > 0.056$ the resistivity in low-T limit is suppressed, which is well correlated with the strong decrease of the R_H at low-T. Both of these effects suggest a reduction of scattering of carriers, possibly by some type of glassy magnetic order which develops in Ni-doped crystals at large y.

In conclusion, we have studied the effect of Co and Ni substitutions on the transport properties of $FeTe_{0.65}Se_{0.35}$ crystals grown with different cooling rates by Brigdman's method. The slow-cooled crystals are inhomogeneous, which affects most properties, while the experiments on fast cooled crystals are most informative. The Hall coefficient, positive in the parent compound, gradually decreases with substitutions, reaching zero at low T at the doping levels $y_{R_H} \approx 0.13$ (Co) and $y_{R_H} \approx 0.056$ (Ni), which is consistent with the electron doping. The T_c is suppressed to zero at $y_c \approx 0.14$ (Co) and $y_c \approx 0.03$ (Ni), suggesting that electron doping may be responsible for the T_c suppression in Co case, while the Ni substitution seems to introduce more complex changes to the system. The low-T upturns, well correlated in ρ and R_H, are observed at small y contents, possibly caused by the scattering of carriers by magnetic fluctuations.

Acknowledgments

We would like to thank M. Kozłowski for experimental support. This work was partially supported by the EC through the FunDMS Advanced Grant of the European Research Council (FP7 Ideas) and by the Polish NCS grant 2011/01/B/ST3/00462. This research was partially performed in the NanoFun laboratories co-financed by the European Regional Development Fund Project POIG.02.02.00-00-025/09.

References

[1] D.C. Johnston, *Adv. Phys.* **59**, 83 (2010).

[2] P.C. Canfield, S.L. Bud'ko, *Annu. Rev. Condens. Matter Phys.* **1**, 27 (2010).

[3] A. Olariu, F. Rullier-Albenque, D. Colson, A. Forget, *Phys. Rev. B* **83**, 054518 (2011).

[4] J. Li, Y.F. Guo, S.B. Zhang, J. Yuan, Y. Tsujimoto, X. Wang, C.I. Sathish, Y. Sun, S. Yu, W. Yi, K. Yamaura, E. Takayama-Muromachiu, Y. Shirako, M. Akaogi, H. Kontani, *Phys. Rev. B* **85**, 214509 (2012).

[5] C. Liu, A.D. Palczewski, R.S. Dhaka, T. Kondo, R.M. Fernandes, E.D. Mun, H. Hodovanets, A.N. Thaler, J. Schmalian, S.L. Budko, P.C. Canfield, A. Kaminski, *Phys. Rev. B* **84**, 020509 (2011).

[6] T. Berlijn, C.H. Lin, W. Garber, W. Ku, *Phys. Rev. Lett.* **108**, 207003 (2012).

[7] F. Nabeshima, Y. Kobayashi, Y. Imai, I. Tsukada, A. Maeda, *Jpn. J. Appl. Phys.* **51**, 010102, (2012).

[8] Z.T. Zhang, Z.R. Yang, L. Li, L.S. Ling, C.J. Zhang, L. Pi, Y.H. Zhang, *J. Phys. Condens. Matter* **25**, 035702 (2013).

[9] T. Inabe, T. Kawamata, T. Noji, T. Adachi, Y. Koike, *J. Phys. Soc. Jpn.* **82**, 044712 (2013).

[10] W. Bao, Y. Qiu, Q. Huang, M.A. Green, P. Zajdel, M.R. Fitzsimmons, M. Zhernenkov, S. Chang, M. Fang, B. Qian, E.K. Vehstedt, J. Yang, H.M. Pham, L. Spinu, Z.Q. Mao, *Phys. Rev. Lett.* **102**, 247001 (2009).

[11] T.J. Liu, J. Hu, B. Qian, D. Fobes, Z.Q. Mao, W. Bao, M. Reehuis, S.A.J. Kimber, K. Proke, S. Matas, D.N. Argyriou, A. Hiess, A. Rotaru, H. Pham, L. Spinu, Y. Qiu, V. Thampy, A.T. Savici, J.A. Rodriguez, C. Broholm, *Nature Mater.* **9**, 716 (2010).

[12] J. Hu, T.J. Liu, B. Qian, Z.Q. Mao, *Phys. Rev. B* **88**, 094505 (2013).

[13] V. Thampy, J. Kang, J.A. Rodriguez-Rivera, W. Bao, A.T. Savici, J. Hu, T.J. Liu, B. Qian, D. Fobes, Z.Q. Mao, C.B. Fu, W.C. Chen, Q. Ye, R.W. Erwin, T.R. Gentile, Z. Tesanovic, C. Broholm, *Phys. Rev. Lett.* **108**, 107002 (2012).

[14] A. Wittlin, P. Aleshkevych, H. Przybylińska, D.J. Gawryluk, P. Dłużewski, M. Berkowski, R. Puźniak, M.U. Gutowska, A. Wiśniewski, *Supercond. Sci. Technol.* **25**, 065019 (2012).

[15] B.C. Sales, A.S. Sefat, M.A. McGuire, R.Y. Jin, D. Mandrus, Y. Mozharivskyj, *Phys. Rev. B* **79** 094521 (2009).

[16] D.J. Gawryluk, J. Fink-Finowicki, A. Wiśniewski, R. Puźniak, V. Domukhovski, R. Diduszko, M. Kozłowski, M. Berkowski, *Supercond. Sci. Technol.* **24**, 065011 (2011).

[17] V.L. Bezusyy, D.J. Gawryluk, M. Berkowski, M.Z. Cieplak, *Acta Phys. Pol. A* **121**, 816 (2012).